Polymerization of sodium-doped liquid nitrogen under pressure

M. M. E. Cormier[1,2] and S. A. Bonev[2,*]
[1]*Department of Physics, Dalhousie University, Halifax, Nova Scotia B3H 3J5, Canada*
[2]*Lawrence Livermore National Laboratory, Livermore, California 94550, USA*
(Received 24 June 2017; published 9 November 2017)

First-principles molecular dynamics (FPMD) simulations are performed on 6 and 12% Na in dense liquid N. A detailed description of structural and electronic properties leading to an understanding of the effect of Na doping on the polymerization phase transition of N is presented. Compression of the mixtures from 5 to 90 GPa shows three distinct regions of characteristic local order separated by pressures near 30 and 65 GPa. Computation of Gibbs free energies of mixing shows that these mixtures are thermodynamically stable beyond 20 and 15 GPa for 6 and 12% Na, respectively.

DOI: 10.1103/PhysRevB.96.184104

I. INTRODUCTION

High pressure (P) and temperature (T) conditions offer unique ways for the synthesis of materials with novel mechanic, optical, and electronic properties. In molecular solids and liquids, the breaking of intramolecular bonds upon compression may lead to the formation of extended (polymeric), covalently bonded structures. The interest in such behavior is partially motivated by the potential discovery of novel energetic materials. Nitrogen, in particular, has become a subject of intense research in recent years. A polymeric structure called cubic-gauche (cg-N), which was predicted [1] among suggestions of possible stable monatomic solid phases [2,3], was eventually synthesized by Eremets *et al.* [4] at P and T above 110 GPa and 2000 K. If polymeric N is recovered to ambient P and T, it would be an energetic material with an energy capacity over five times greater than current energetic materials [4]. However, attempts to quench cg-N to ambient conditions [5–7] have been unsuccessful to date.

A possible route to metastable N is to tune the polymerization transition by combining (doping) N with small amounts of other elements. Indeed, in order to discover energetic materials with optimal properties, it is essential to explore bonding and structural properties as a function of all three fundamental variables:- pressure, temperature, and chemical composition. Here optimal properties include metastability at ambient conditions, polymerization transition at relatively low pressure, and high energy capacity. The last requirement suggests a focus on N-rich systems with small amounts of dopants. Additionally, the fact that in experimental settings molecular-to-polymeric transitions are usually observed at high T means that it is critical to understand the evolution with pressure of bonding and structural properties of molecular compounds at elevated temperatures.

Achieving these goals is challenging for a number of reasons: (i) the extreme complexity of the phase diagrams of s-p-valent materials, including numerous phases and extended regions of metastability, (ii) limitations of *in situ* measurements at high-P and T, and (iii) limitations of theoretical techniques for structure searches at high T and large crystalline unit cells (small dopant concentrations). Perhaps for these reasons, studies to day [8–12] have focused mostly on compositionally simple systems, and even their finite-T phase diagrams are not entirely known yet.

Here we have taken an alternative approach to study polymerization in N-rich systems. Investigations of liquids provide a direct way of studying the evolution of bonding properties with density at finite temperature, while avoiding many of the difficulties associated with global phase space searches of crystalline stability. The relevance of these findings for the problem of crystalline stability is grounded on the established parallels between solid and liquid structures under pressure [13–16]. The case of N is particularly favorable because of the existence of a sharp, first order liquid-liquid phase transition with well-defined structural changes [15].

In this paper, we report results on the polymerization of liquid N doped with Na. First principles molecular dynamics (FPMD) simulations are used to collect statistical information about the liquid as a function of pressure for different Na concentrations. Their structural, electronic, and thermodynamic properties are characterized, based on which distinct transition stages are identified. Our results show that only a small concentration of Na (a few %) is required to induce polymerization at sufficiently lower pressure compared to the pure N system. The properties of the pure and doped systems are compared and contrasted.

II. COMPUTATIONAL METHODS

FPMD simulations of liquid N mixed with 6 and 12% Na, as well as pure N and pure Na, have been performed for pressures between 15 and 100 GPa along their respective 2000 K isotherms using finite-temperature density functional theory (DFT) [17] within the Perdew-Burke-Ernzerhof generalized gradient approximation (PBE-GGA) [18] as implemented in the Vienna *ab initio* simulation package (VASP) [19]. The FPMD simulations were carried out in the canonical (constant number of particles N, volume V, and temperature T) ensemble using Born-Oppenheimer dynamics and a Nosé-Hoover thermostat. Supercells with periodic boundary conditions of 128 atoms were used for the Na-N mixtures and for pure liquid N, while 64 atom supercells were used for pure liquid Na. The supercells were initially randomly populated with N_2 molecules and the appropriate concentration of isolated Na atoms while enforcing a minimum separation between

*bonev@llnl.gov

molecules and Na atoms. The Na concentration is measured as the ratio of the Na atoms to the total number of atoms in the system. Before compression, the composition of the liquids was confirmed to be made of molecular N_2 with isolated Na atoms.

To obtain well-converged pressures (within ∼0.1 GPa) and energies (∼1 meV/atom), the Brillouin zone was efficiently sampled using a single **k** point at $(\frac{1}{4},\frac{1}{4},\frac{1}{4})$ in the Brillouin zone. Convergence tests with up to $3 \times 3 \times 3$ uniform **k**-point meshes were carried out over a wide range of pressures and temperatures. Using a 0.5 fs ionic time step, each FPMD trajectory was first equilibrated within 2–3 ps and continued for an additional 5 ps from which structural, electronic, and thermodynamic properties were calculated. Nine- and five-electron projector augmented wave (PAW) pseudopotentials (PP) with 2.2 and 1.6 Bohr core radii were used for all Na and N calculations, respectively, using a 600 eV plane-wave cutoff energy.

For accurate determination of free energies of mixing, the PBE-GGA energies and pressures were corrected using the HSE06 hybrid functional of Heyd, Scurseria, and Ernzerhof [20]. This was done on isolated atomic configurations taken from the FPMD trajectories. The resulting corrections were averaged over the sampled snapshots. We found that five well-separated configurations from a given trajectory are sufficient to converge the average corrections for all pressures considered. The fluctuations in the energy corrections were negligible (on the order of 10^{-3} meV/atom), indicating that the PBE-GGA ensemble is sufficient.

III. RESULTS

Upon compression, the Na-N mixtures with 6 and 12% Na concentration exhibit three distinct regions with characteristic local structural order emerging at concentration-dependent pressures. In Sec. III A we describe in detail the case of 12% Na and present partial results for 6% Na, noting that the two cases are qualitatively similar. However, we find that the systems with larger Na concentration considered here, 25 and 50%, are significantly different. These differences, both structural and electronic, require special attention and will be described in a follow-up article.

The structural analysis allows for informative decomposition of the electronic properties of the liquids among characteristic clusters. The electronic properties described in Sec. III B elucidate the effect of Na doping on the evolution of bonding properties of N as a function of compression. Finally, thermodynamic stability as a function of concentration is analyzed for the entire pressure range considered, and concentration-dependent equations of state are presented in Sec. III C.

A. Structural properties

For the case of 12% Na, structural transitions occur near 30 and 65 GPa. These pressures mark the appearance or disappearance of some characteristic features in the local order, while compression within each region yields gradual progression of structural properties with no qualitative changes.

The initial step in the structural analysis is to calculate the distribution of nearest neighbor (n.n.) species around each atom in the supercell for every time step in the simulation trajectories. These data are used to identify distinctive atomic arrangements within the liquid—their composition, geometry, and temporal stability.

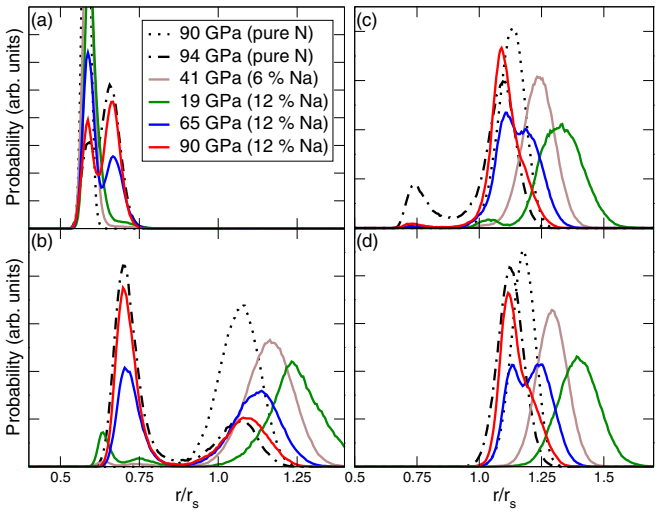

FIG. 1. Probability distribution of density-rescaled distances for the (a) first, (b) second, (c) third, and (d) fourth N-N nearest neighbors. Results are shown for liquids with 12% and 6% Na concentrations and for pure N at several pressure as indicated in the legend. The structural changes in the two doped systems are qualitatively similar but commence at higher pressure and are less pronounced with the smaller Na concentration.

We found that the transitions are clearly marked by distinct features in the first to fourth N-N n.n. distance distributions (n.n.d.d.). Figure 1 shows a histogram of N-N neighbor distances, rescaled by the density parameter r_s, in order to facilitate comparison between structural properties at different pressures. Here r_s is defined by $4/3\pi r_s^3 = V/N$; notice that N is the number of ions, not electrons. An appropriate cutoff radius R_c was determined as the first minimum of the N-N pair correlation function, from which coordination fractions were determined as ensemble averages. Using this information, we define a molecule (N_2) as two atoms that are mutual nearest neighbors and both are singly coordinated (within the cutoff radius). An n-atom N ring (N_n ring) is identified as a closed sequence of n 2-coordinated atoms. An n-atom N chain (N_n chain) is located by searching for a sequence of $(n-2)$ 2-coordinated atoms terminating on each end with atoms which are c-coordinated, where $c \neq 2$. Notice that with these definitions, if a cluster is formed by attaching an N_n ring to an N_m chain, the cluster will be identified as an N_m chain.

First, the region below 30 GPa is characterized by a broadened peak with a shoulder in the first n.n.d.d. and two small peaks in the second n.n.d.d. The peak in the first n.n.d.d. is due to N_2 molecules, the broadening comes from the first neighbor in N_3 chains (azide), and the shoulder corresponds to N_4 rings. The N_3 chains yield the first peak in the second n.n.d.d., while the second peak is due to the formation N_4 rings. The N_2 molecules have an equilibrium bond distance very close to 1.1 Å in agreement with the chemical bond distance of isolated N_2 molecules. The N_3 chains have bond

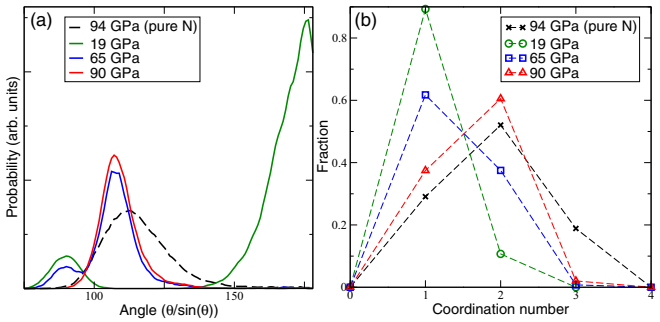

FIG. 2. (a) N-N-N angle distributions and (b) N-N coordination numbers for 12% Na concentration in liquid N. The angle distributions are calculated by taking into account only the first two N n.n. within a distance less than the appropriate cutoff radius R_c for the given pressure (see text). The N-N coordination numbers are calculated based on the ensemble-averaged number of N atoms found within R_c.

distances between 1.15 and 1.25 Å, and the N-N-N angle is nearly flat with a peak near 180 degrees (see Fig. 2) in accordance with double-bonded azide chains. The N_4 rings are bonded with distances between 1.25 and 1.35 Å as is the case in the tetra-nitrogen molecule, corresponding to double and single bonds, and are very close to square with a peak in the N-N-N angle near 90 degrees. Thus, at pressures up to 30 GPa, even though there is a small fraction of broken N_2 molecules, the species that appear in the liquid are known from ambient-P chemistry.

Compression beyond 30 GPa causes N_3 chains to bond with N_2 molecules forming N_5 rings. This is marked by the splitting of the first n.n.d.d., the heightening of the first peak in the second n.n.d.d., and the splitting of the peak in the third and fourth n.n.d.d. The emergence of a peak at about 108 degrees in the angle distribution also marks the formation of N_5 rings. The fraction of these rings increases with pressure while the fraction of N_3 chains decreases proportionally to the fraction of N_2 molecules (see Fig. 3). The N_4 rings persist in this pressure region. The bond distances in the N_5 rings are between 1.25 and 1.35 Å consistent with the lengths of double and single N-N bonds.

Further compression past 65 GPa yields N chains longer than N_3 while the fraction of N_5 rings continues to increase. The fraction of N_3 chains becomes negligible by 65 GPa as is marked by the disappearance of the first small peak in the 2nd n.n.d.d. and the disappearance of the peak at about 170 degrees in the angle distribution. The fraction of N chains longer than N_3 in this region becomes finite but N chains of any length possess the same N-N bond lengths, between 1.25–1.35 Å, and have the same peak in the N-N-N angle distribution, at 108 degrees, as the N_5 rings. Thus, in this third region, N_3 chains, N_n chains with $n > 3$, and N_5 rings cannot be distinguished based on the n.n.d.d. and N-N-N angles; coordination analysis must be used to explicitly search for each cluster type. This analysis also shows that N chains in this region emerge as tails of N_5 rings where one terminal N is 3-coordinated as a member of both a ring and a chain and the other terminal N singly coordinated. The complete disappearance of N_4 rings does not occur until 75 GPa.

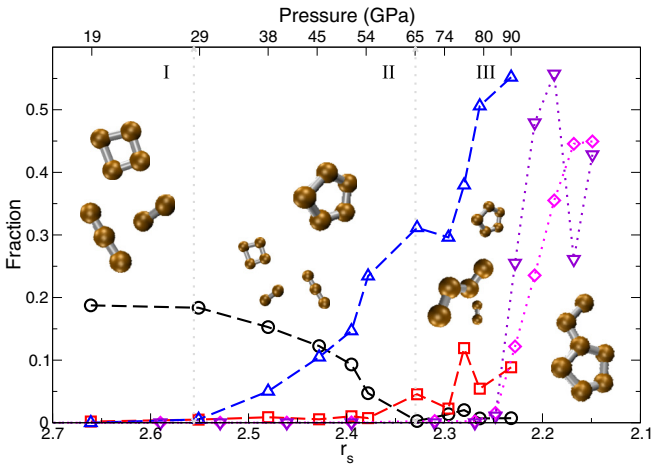

FIG. 3. The fraction of the total number of N atoms which form N_3 chains in liquid N with 12% Na (black-dashed circles), N_4 to N_8 chains in 12% Na (red-dashed squares) and in pure N (magenta-dotted diamonds) liquids, and N_5 rings in 12% Na (blue-dashed up-triangles) and in pure N (violet-dotted down-triangles). The ball-and-stick representations show characteristic clusters present in each of the three regions.

It is important to note the persistence of N_5 rings in the Na doped systems compared to pure N. Thus even though the polymerization in the former commences at lower pressure, the latter has a larger fraction of single-bonded three-coordinated N atoms at pressures above 90 GPa.

B. Electronic density of states

The electronic density of states (EDOS) are obtained from the charge density of atomic configurations taken from the FPMD trajectories. For liquids, the ensembles are sampled and the results are averaged. In our case, we found that taking five snapshots is sufficient to obtain converged EDOS averages. For each static calculation, the Brillouin zone was sampled efficiently with 4 **k** points at $(\frac{1}{4},\frac{1}{4},\frac{1}{4})$, $(\frac{1}{2},\frac{1}{4},\frac{1}{4})$, $(\frac{1}{2},\frac{1}{2},\frac{1}{4})$, and $(\frac{1}{2},\frac{1}{2},\frac{1}{2})$, which were given weights 1, 3, 3, and 1, respectively. This sampling approach produces better results than a uniform $3 \times 3 \times 3$ mesh and completely reproduces converged results obtained with uniform $4 \times 4 \times 4$ and $6 \times 6 \times 6$ **k**-point grids. The EDOS are projected on the N and Na species (Fig. 4) and further decomposed based on the types of clusters that the atoms are part of (Fig. 5). Site projections were obtained by choosing a cutoff radius of half the first coordination shell radius. As a consequence, small overlaps were incurred, but features from higher energy states that were otherwise missed became apparent.

At 19 GPa (region I of the doped system with 12% Na) pure N is still an insulator with a band gap of about 5 eV. The Na atoms contribute electronic states in this band gap region. As a result, there is a small amount of occupied states at the Fermi level of the Na-doped system—partial occupancy of the antibonding orbitals of the N_2 molecules. Furthermore, additional EDOS appear below the Fermi level, which belong mostly to N_3 chains. These are formed with extra electronic charge transferred from the Na atoms. Meanwhile, the valence states due to N_2 molecules remain very similar to those in pure

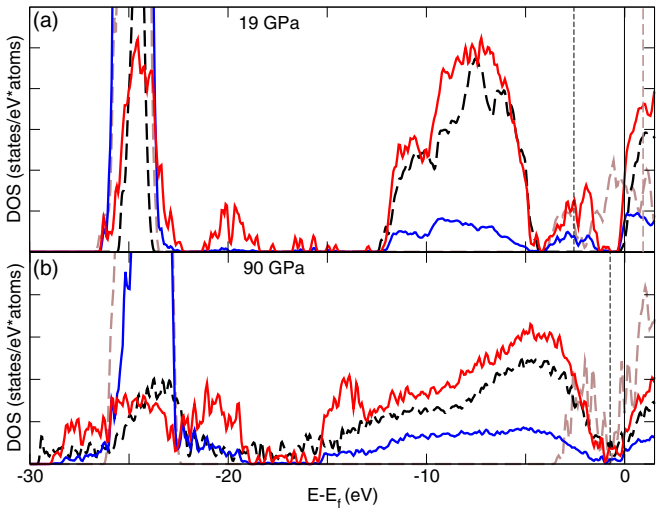

FIG. 4. Site-projected electronic density of states (EDOS) for 12% Na in liquid N showing the N (red) and Na (blue) projections along with pure N (black dashed) and pure Na (brown dashed) for (a) 19 GPa and (b) 90 GPa. The pure systems EDOS were shifted relative to their Fermi levels to show similarities in profiles with the mixtures. The respective Fermi levels are shown by vertical lines for the mixtures (black-solid), pure N (black-dashed), and pure Na (brown-dashed).

liquid N. The molecular states around −30 eV are broadened compared to the pure case and the appearance of states around −20 eV are strictly due to N_3 chains. As seen in Fig. 5, the EDOS of the 6 and 12% Na systems are qualitatively similar; the difference is that in the former the peak below the Fermi level associated with the azide chains is less pronounced as there are less of them.

With increasing density, the edge of the valence molecular states is broadened towards the Fermi level until it overlaps with the N_3 states in the gap. At this point, around 30 GPa, the

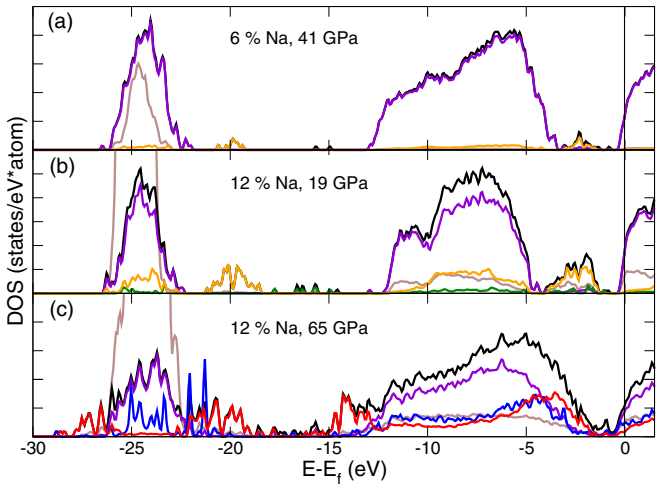

FIG. 5. Cluster decomposition of the electronic density of states (EDOS) for liquid N with 6% and 12% Na, showing N_3 chains (orange), N_2 molecules (violet), N_4 rings (green), 5-member N-rings (red), n-member N-chains, $n \geqslant 3$ (blue), and the total site-projected EDOS for N (black) and Na (brown).

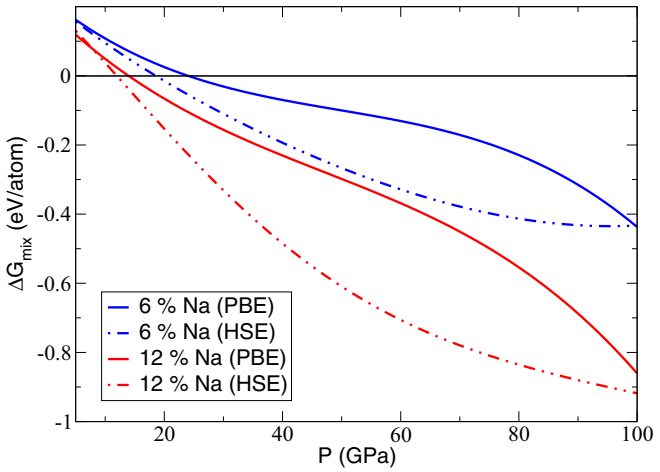

FIG. 6. Gibbs free energies of mixing as a function of pressure with (dotted-dashed) and without (solid) HSE corrections for 6 and 12% Na in liquid N.

formation of 5-member N rings, by combining N_2 molecules with N_3 chains, is possible. As more rings form, the states within the gap are completely overtaken. Notice that states owing to n-member chains ($n \geqslant 3$) are nearly identical to 5-member rings, except for the lower energy stabilizing states around −14 eV.

Compression beyond 65 GPa into region III (of the 12% Na system) yields no qualitative changes in the electronic structure. The fraction of N_2 molecules decreases and so the total number of states due to various clusters changes, but there is no qualitative change in the profile of the EDOS.

We see that the mechanism of polymerization here is different than in pure N where the molecules remain stable until the electronic band gap closes at around 90 GPa and the liquid becomes metallic. Small amounts of Na are sufficient to change significantly the electronic structure of the liquid by facilitating the formation of N_3 chains with states in the band gap. The latter become precursors for the breaking of the already weakened N_2 molecules due to occupancy of antibonding orbitals leading to the formation of poly-N at pressures much lower than 90 GPa.

C. Free energy of mixing and equation of state

Here we examine the thermodynamic stability of the liquids by computing their Gibbs free energies. Pressures, temperatures, and energies were calculated from ensemble (time) averages, while entropies were determined following the method outlined in Ref. [21]. We then calculate the Gibbs free energies of mixing of the liquids from $\Delta G_{\text{mix}} = G_{(N-Na)_i} - x_i G_N - (1 - x_i) G_{Na}$, where x_i is the concentration of N in mixture $(N - Na)_i$ and each G_X term on the right hand side is the Gibbs free energy per atom of liquid X.

The results in Fig. 6 show that the mixtures are thermodynamically stable with respect to the pure systems beyond a maximum of ∼23 GPa. Hybrid functional corrections are shown to be largest in the transition region, but yield corrections in favor of the mixtures.

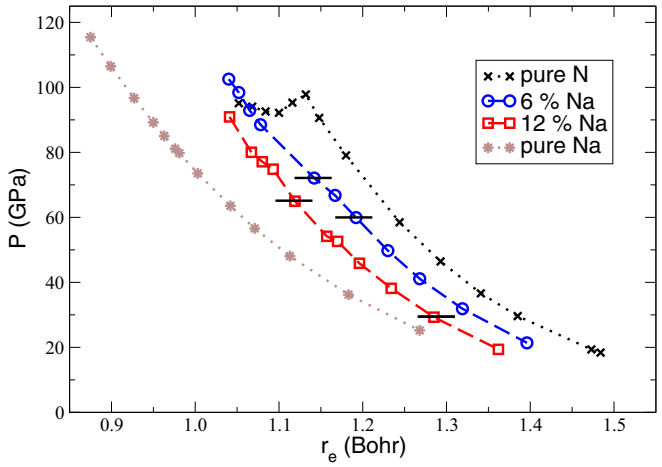

FIG. 7. Equations of state. The pressure is plotted against the valence electron density r_e (see text for details).

The equations of state for pure liquid N, N mixed with 6, and 12% Na, and pure liquid Na are shown in Fig. 7. The pressure is plotted against the valence electron density parameter, r_e, defined as $V_e/N_e = (4/3)\pi(r_e a_0)^3$. Here $V_e = V - V_{\text{ion core}}$, where $V_{\text{ion core}}$ is the volume assigned to atomic cores. It is calculated by taking the core radius as the Wigner-Seitz radius from the pseudopotentials. N_e is the number of valence electrons implemented in the pseudopotentials, and a_0 is the Bohr radius. At the same pressure, the valence electron density increases with Na-doping concentration. Thus, the Na subsystem chemically compresses the N subsystem, catalyzing the formation of 5-member N rings and n-member chains, $n \geqslant 3$.

IV. CONCLUSION

We have characterized the structural, electronic, and thermodynamic properties of Na-doped liquid N as a function of pressure. The polymerization transition develops in three stages and commences at much lower pressures compared to the pure N system even with small Na concentrations. We have elucidated the mechanism by which Na promotes this transition.

In the case of pure liquid N, the valence states are broadened upon compression, where at the transition pressure the system metallizes, destabilizing N_2 molecules. For the mixtures at low pressure, the presence of additional electrons from Na destabilizes N_2 bonds by shifting the Fermi level and populating antibonding orbitals allowing the formation of N_3 azide chains. Assisted by the chemical compression owing to Na ions, the valence states of N_2 molecules are broadened upon compression, overlapping with the midgap states of the N_3 chains, yielding the preferred N_5 rings. Further compression gradually breaks N_2 molecules forming additional N_5 rings and N chains of length 3 or greater. The role of Na is then twofold: to provide additional electrons that destabilize molecular bonds and to chemically compress the N subsystem, yielding a second-order phase transition that does not fully metallize at high P. This is in contrast to the first-order liquid-liquid phase transition of pure liquid N induced by metallization.

ACKNOWLEDGMENTS

Work performed under the auspices of the US Department of Energy under Contract No. DE-AC52-07NA27344. Computational resources were provided by Acenet and Livermore Computing.

[1] C. Mailhiot, L. H. Yang, and A. K. McMahan, Phys. Rev. B **46**, 14419 (1992).
[2] A. K. McMahan and R. LeSar, Phys. Rev. Lett. **54**, 1929 (1985).
[3] R. M. Martin and R. J. Needs, Phys. Rev. B **34**, 5082 (1986).
[4] M. I. Eremets, A. G. Gavriliuk, I. A. Trojan, D. A. Dzivenko, and R. Boehler, Nat. Mater. **3**, 558 (2004).
[5] T. W. Barbee III, Phys. Rev. B **48**, 9327 (1993).
[6] T. Zhang, S. Zhang, Q. Chen, and L. M. Peng, Phys. Rev. B **73**, 094105 (2006).
[7] X.-Q. Chen, C. L. Fu, and R. Podloucky, Phys. Rev. B **77**, 064103 (2008).
[8] B. A. Steele and I. I. Oleynik, Chem. Phys. Lett. **643**, 21 (2016).
[9] B. A. Steele and I. I. Oleynik, J. Chem. Phys. **143**, 234705 (2015).
[10] X. Wang, J. Li, H. Zhu, L. Chen, and H. Lin, J. Chem. Phys. **141**, 044717 (2014).
[11] X. Wang, J. Li, J. Botana, M. Zhang, H. Zhu, L. Chen, H. Liu, T. Cui, and M. Miao, J. Chem. Phys. **139**, 164710 (2013).
[12] M. I. Eremets, M. Y. Popov, I. A. Trojan, V. N. Denisov, R. Boehler, and R. J. Hemley, J. Chem. Phys. **120**, 10618 (2004).
[13] I. Tamblyn, J.-Y. Raty, and S. A. Bonev, Phys. Rev. Lett. **101**, 075703 (2008).
[14] I. Tamblyn and S. A. Bonev, Phys. Rev. Lett. **104**, 065702 (2010).
[15] B. Boates and S. A. Bonev, Phys. Rev. Lett. **102**, 015701 (2009).
[16] B. Boates and S. A. Bonev, Phys. Rev. B **83**, 174114 (2011).
[17] W. Kohn and L. Sham, Phys. Rev. **140**, A1133 (1965).
[18] J. P. Perdew, K. Burke, and M. Ernzerhof, Phys. Rev. Lett. **77**, 3865 (1996).
[19] G. Kresse and J. Hafner, Phys. Rev. B **47**, 558 (1993); Comp. Mat. Sci. **6**, 15 (1996).
[20] J. Heyd, G. E. Scuseria, and M. Ernzerhof, J. Chem. Phys. **124**, 219906 (2006).
[21] A. M. Teweldeberhan and S. A. Bonev, Phys. Rev. B **83**, 134120 (2011).